

Two Fuel Cell Cars In Every Garage?

by Mark F. Mathias, Rohit Makharia, Hubert A. Gasteiger, Jason J. Conley, Timothy J. Fuller, Craig J. Gittleman, Shyam S. Kocha, Daniel P. Miller, Corky K. Mittelsteadt, Tao Xie, Susan G. Yan, Paul T. Yu

In 1928, U.S. presidential candidate Herbert Hoover promised growing prosperity represented by “a chicken in every pot and two cars in every garage”. We now find ourselves at a point in history wondering if and when the power for those cars will come from fuel cells instead of internal combustion engines. The answer to those questions depends largely on two key materials on which the success of the technology hinges – namely, the membrane and the electrocatalyst.

Over the past decade, significant R&D progress has been made toward meeting the challenging cost and performance targets required for the use of polymer electrolyte fuel cells (PEFCs) in automotive applications. The catalyst and membrane are incorporated into a membrane electrode assembly (MEA), and MEA optimization has been a critical element of this progress. Platinum loadings have been reduced from several $\text{mg}_{\text{Pt}}/\text{cm}^2_{\text{MEA}}$ ¹ to values of 0.5-0.6 $\text{mg}_{\text{Pt}}/\text{cm}^2_{\text{MEA}}$ in current applications and loadings as low as 0.25 $\text{mg}_{\text{Pt}}/\text{cm}^2_{\text{MEA}}$ have been demonstrated on the research level.² Furthermore, implementation of thin membranes (20-30 μm)^{3,4} as well as improvements in diffusion medium materials, have essentially doubled the achievable MEA power density to ca. 0.9 $\text{W}/\text{cm}^2_{\text{MEA}}$ (at 0.65 V),⁵ thereby not only reducing the size of a PEFC system, but also reducing its overall materials cost (controlled to a large extent by membrane and Pt-catalyst cost). In this article, an update on our paper of similar scope from one year ago,⁶ we evaluate current cost, performance, and durability issues associated with PEFC membranes and catalysts, and we suggest areas where a renewed focus of R&D effort will accelerate the commercialization of PEFCs in automotive applications. We invite the increased participation of material developers to join the

growing effort to realize the fuel-cell version of Hoover’s promise.

Membrane Cost

The current polymer electrolyte fuel cell membranes of choice are based on poly[perfluorosulfonic acid] (PFSA), and are produced by DuPont, Asahi Glass, Asahi Kasai,

Solvay, and 3M. Although PFSA is also typically used as a binder in electrode layers, this cost impact is small relative to the membrane which requires approximately 10 times more PFSA. PFSA membrane has been commercialized for the chlor-alkali industry, but the market volume is small (<65 metric tons (MT)/year)⁷ and the current price is high ($\approx \$5,000/\text{kg}$, $\approx \$250/\text{m}^2$ as finished 25 μm fuel cell membrane), characteristic of a specialty material. This compares with the commodity poly[tetrafluoroethylene] which is produced at a volume of 80,000 MT/year and sells in the neighborhood of $\$10/\text{kg}$. To assess the high-volume automotive price potential of PFSA membrane, we conducted a study for cost estimation purposes to produce vinyl ether monomer, PFSA polymer, and membrane. The price projections are shown in Fig. 1 and indicate that at 1 million vehicles/yr (less than 2% of world market), which would require approximately 15 million m^2/yr of membrane (100 kW/vehicle at 15 $\text{m}^2/\text{vehicle}$), the membrane cost would drop to well less than $\$10/\text{m}^2$ ($\$200/\text{kg}$). This translates to approximately $\$1.5/\text{kW}$, becoming an affordable price against a fuel cell engine target in the neighborhood of $\$25/\text{kW}$, and demonstrates that the PFSA price should not be prohibitive for wide-scale automotive application. Price projections from DuPont for 25 μm membrane based on 2004 membrane technology,⁸ while a factor of about

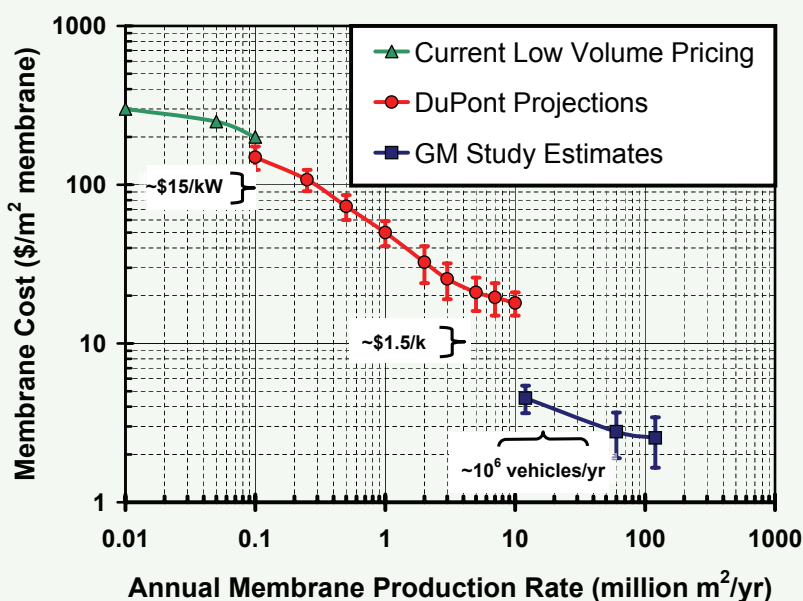


Fig. 1. Price projection of PFSA membrane (25 μm thick, 0.05 kg/m^2 , 1,100 EW) at high volume. Intermediate-volume projections provided by DuPont.⁸ High-volume numbers from GM cost study. Error bars indicate rough uncertainty on projections.

four higher than our study results at 10 million m²/yr, are qualitatively consistent with this assessment. One reason for the discrepancy between the two projections is that the GM study was done assuming construction of a new high volume plant and thus did not account for the financial burden of having to ramp up to that volume over time.

Although the price of PFSA may become affordable in the neighborhood of one million vehicles/year, there are reasons to work on the development of alternative (e.g., hydrocarbon) membranes. The primary motivations are (1) the possibility of decreased membrane cost at lower automotive volumes, (2) the elimination of fluoride to decrease metal plate corrosion problems, thus enabling the use of more affordable plate materials, and (3) the need for materials with improved conductivity at low (e.g., 25-50%) relative humidity (RH), the subject of the next section.

Membrane Performance

Our suggested development priorities in the area of membrane performance are in order of importance: (1) improved low-RH conductivity at operating temperatures of 60-80°C, (2) low water uptake in automotive operation (which includes the presence of liquid water), and (3) high temperature (120°C) operation at 25% RH or less. We address these issues in order below.

Low-RH conductivity. – Current PEFC systems run at a maximum of 80°C because operation above that temperature requires too much system support of the membrane (e.g., pressure, humidification) to maintain close to 100% RH required for good proton conduction. Also, current membranes have glass transition temperatures in the range of 80-120°C and are thus subject to creep and hole-formation at temperatures in that range. Figure 2a shows the conductivity vs. RH for a Nafion[®] 1,100 EW (EW = $\frac{g_{\text{polymer}}}{\text{mol}_{\text{H}^+}}$) membrane at 80°C, and this response is not sensitive to temperature up to 120°C.⁹ At the fully humidified condition, the conductivity of approximately 0.1 S/cm translates to a tolerable 25 mV loss for a 25 μm membrane at a current density of 1 A/cm². Figure 2a also shows that the conductivity drops off quickly with RH, thereby requiring the fuel cell system to provide for humidification of the reactant streams. There would be great value in reducing system

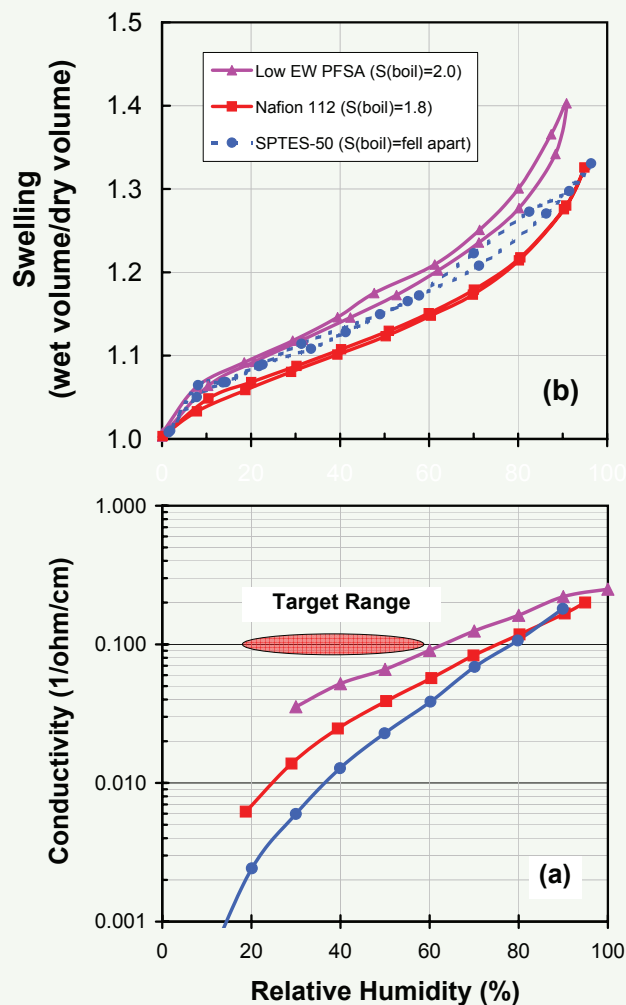


Fig. 2. (a) Conductivity vs. RH at 80°C for Nafion[®] 112, SPTES at 1.8 meq/g,¹⁰ and low EW (<800) PFSA. Also indicated are desired conductivity characteristics to enable system simplification and vehicle heat rejection. (b) Membrane swelling at 80°C. Legend lists swelling when membranes were boiled in liquid water.

complexity (and thus cost) from a membrane that maintains good conductivity to low RH such as shown in the target region in Fig. 2a (0.1 S/cm at 25-50% RH), even if operated at 60-80°C with occasional excursions to 100°C. Developments by manufacturers have shown promising progress in this direction for PFSA membranes. An example is shown in Fig. 2a, a low (<800) EW PFSA that has conductivity of 0.06-0.07 S/cm at 50% RH and 80°C. Also shown in Fig. 2b are data from a sulfonated polyaryleneethioethersulfone (SPTES-50, 1.8 meq/g) described by Dang and co-workers¹⁰ and synthesized in our lab. This conductivity vs. RH performance is a characteristic of many hydrocarbon membranes — it surpasses Nafion[®] 112 at high RH (>80%) but drops off more sharply than Nafion[®] 112 as the RH is decreased.

Water uptake. – In addition to the membrane proton conductivity vs. RH relationship as a measure of system compatibility, it is important to consider the water uptake vs. RH characteristic. In an automotive application, we anticipate that a membrane will be exposed to environments ranging from contact with liquid water to contact with dry gas at approximately 80-100°C. Figure 2b shows the water uptake as a function of RH for the three membranes for which conductivity data are shown. The results in Fig. 2b were obtained using an environmentally controlled Rubotherm balance and then translating the weight to swelling using the membrane dry density and assuming no free volume in the dry membrane. We observe that in subsaturated conditions, the

(continued on next page)

SPTES membrane swells about the same amount as the low-EW PFSA membrane at a given RH. Both these membranes swell approximately 40% more at a given RH than Nafion® 112.

The legend of Fig. 2b also indicates water uptake data obtained by boiling the three membranes in liquid water for 1 h. When in contact with boiling water, the PFSA membranes swell to close to a factor of 2 over the membrane dry volume, whereas the SPTES membrane expands so much that it falls apart. High membrane volume swell is difficult to manage from a stack compression viewpoint, as it tends to over-compress and damage the diffusion media.⁵ Large water uptake is also undesirable because of the fatigue impact of shrink-swells due to automotive RH cycling, as further discussed below in the section on membrane mechanical durability.

Based on the above arguments, we prefer a membrane that offers as much conductivity as possible with minimal water uptake. Figure 3 is a plot of membrane conductivity vs. membrane swelling, derived from the data in Fig. 2. It shows that the two PFSA membranes exhibit the same relationship, whereas the SPTES membrane swells significantly more at a given conductivity. This suggests that the SPTES uses water less efficiently than the PFSA materials, implying that the conductivity vs. water uptake and/or the percolation behavior of the PFSA are favorable compared to the SPTES membrane.

Whereas Fig. 2a indicates system compatibility, Fig. 3 indicates

membrane material utility and viability. Based on our experience to date, we estimate an upper limit that a membrane material can swell is a factor of 2 (vs. dry) when placed in boiling water for 1 h. Beyond that, the difficulty of managing the swelling on internal stack forces and/or on the membrane itself (as described below) is prohibitive.

High-temperature membranes.—Unfortunately, the heat rejection rate of current automotive radiators is insufficient to reject continuous full-power waste-heat loads with the 80°C fuel cell stack temperature. Operation at 80°C results in significant adjustment in thermal system complexity/cost, vehicle design, and/or negative impact on the high-power vehicle capability (e.g., length of time at full load). Vehicle system analysis indicates that 120°C high-power operation would enable the use of radiators similar to those available today,¹¹ and this has driven the need for development of a high-temperature membrane that can operate at temperatures up to 120°C. Earlier we argued that such a membrane must have a conductivity of 0.1 S/cm at 25% RH in order not to increase system-support demands over those of state-of-the-art membranes.⁵ This has led to development projects focused on high-temperature (120°C), low-RH (25%) membranes.

In our last paper on membrane requirements,⁶ we expressed concern about the impact of extended operation at 120°C on Pt cathode catalyst dissolution. Based on new data to be presented here, we argue in the Electrocatalyst durability section below that this concern is valid only for well-humidified systems. We now believe a 120°C system at 25% RH

is desired for system simplification and feasible from a catalyst durability viewpoint.

In the absence of higher temperature membranes, operation is limited to 80°C and results in heat rejection systems for fuel cell vehicles that are more complex than in current automotive applications. This in turn drives for a more aggressive simplification of the fuel cell system, achievable, for example, by the development of low-RH membranes which would enable stack operation at 80°C without external humidification. Thus, the development of low-RH (0.1 S/cm at 25-50% RH) membranes with a main operating temperature of 60-80°C is an important intermediate target on the way to the ultimate goal of low-RH (0.1 S/cm at ≤25% RH) membranes operating at 120°C.

Phosphoric acid-doped polybenzimidazole (PBI), first identified by Case Western Reserve University (an extension of this technology is now under development by PEMEAS GmbH), is a high temperature membrane that allows operation up to approximately 200°C with low humidification requirement.¹² However, issues that are barriers to its use for automotive applications are instability in the presence of liquid water and inefficient cathode structures resulting in low areal power density.

Whereas much work is ongoing to develop alternative membranes to PFSA, the vast majority of approaches rely on the sulfonic acid based conduction mechanisms. Fundamental work such as morphological investigations¹³ and molecular modeling are needed to determine the physical limits of these materials in terms of conductivity vs. RH characteristic shown in Fig. 2. Also, the data in Fig. 2 and 3 suggest that PFSA may have an intrinsic morphological advantage at low RH over the hydrocarbon materials, and this requires investigation at the fundamental level.

Membrane Durability

To be successful in automotive application, membranes must survive 10 years in a vehicle and 5,500 h of operation including transient operation with start-stop and freeze-thaw cycles. Even though thin polymer electrolyte membranes (20-30 μm) enable high power density operation, the requirements on their chemical and mechanical stability are significantly more demanding

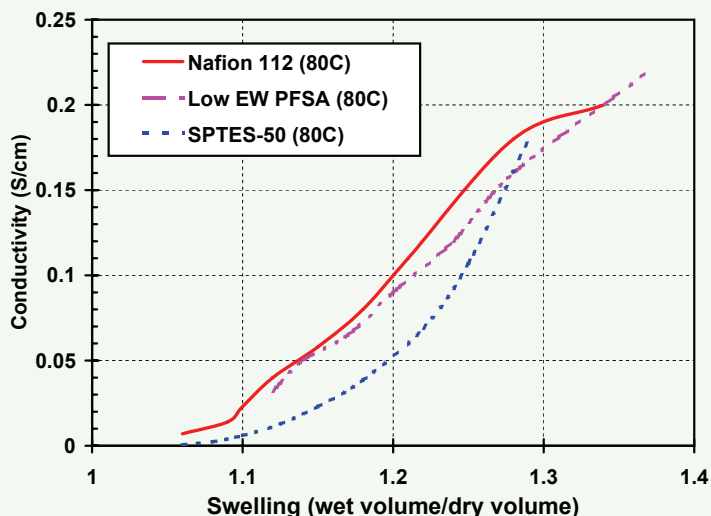


FIG. 3. Membrane proton conductivity vs. swelling for membranes shown in Fig. 2.

compared to those imposed on 100–200 μm membranes used in the past.

While PFSA membranes are chemically stable, they are known to degrade in the fuel cell environment⁴ via peroxy-radical attack, strongly enhanced in the presence of trace iron contamination.¹⁴ Success of PEFC technology requires understanding and mitigation of the PFSA chemical degradation mechanism. The mechanism is complicated, depending on ionomer structure, iron level, catalyst components, electrode design, relative humidity, temperature, and other factors. Fortunately, several research groups are focused on understanding this mechanism, and good progress is being made.^{15–17} Accelerated tests useful for membrane development typically include operation at open circuit voltage, low RH (25–50%), and elevated temperature (80–95°C).¹⁶

As discussed above, membranes swell when soaked in water and subsequently shrink during drying. A constrained membrane experiences in-plane compression during swelling under wet conditions and in-plane tension due to shrinkage under dry conditions.¹⁸ Cycling between these compressive and tensile states creates fatigue that may eventually lead to fracture of the membrane. Additionally, membranes exhibit viscoelastic creep to relieve these

stresses, and this may eventually lead to pinholes due to local thinning. As a demonstration of this purely mechanical failure mode, Fig. 4 shows a leak developing in an RH-cycling test for a MEA made from a cast 25 μm Nafion[®] membrane (NR111). The 50 cm^2 MEA was cycled between 150% RH for 2 min and 0% RH for 2 min at 80°C under air/air to study mechanical failure of membranes in absence of chemical degradation. Membrane failure was monitored by membrane gas crossover leaks measured via air permeation at an applied differential pressure of 20 kPa (in units of standard cm^3 per minute (sccm), with an end-of-life criterion of 10 sccm). Although an automotive fuel cell system is not expected to experience such harsh RH cycling, this test has been useful in screening membrane materials for mechanical properties. Some PFSA membranes have lasted more than 20,000 cycles without failure. Figure 4 also includes a typical example with a hydrocarbon membrane. Aromatic hydrocarbon membranes tested to date last no more than 300 cycles as they appear to undergo embrittlement after relatively few wet-dry cycles.

More work is needed to understand the connection between these *ex situ* mechanical properties and *in situ* failure. Clearly, dimensional stability and limited water uptake in liquid water (less than a factor of

2 swelling maximum) are desirable. To support such efforts, an improved fundamental understanding of the morphology of these materials both through experiments [e.g., small angle X-ray scattering (SAXS), small angle neutron scattering (SANS)] and molecular modeling is needed.

Electrocatalyst Cost and Performance

Due to the fast H_2 oxidation kinetics on carbon supported Pt catalysts (Pt/C), anode Pt loadings can be lowered to 0.05 $\text{mg}_{\text{Pt}}/\text{cm}^2$ without performance loss.² However, the slow O_2 reduction kinetics still require cathode Pt-loadings of ≈ 0.4 $\text{mg}_{\text{Pt}}/\text{cm}^2$ to meet energy efficiency (*i.e.*, cell voltages of ≈ 0.65 V) and MEA power density (*i.e.*, P_{MEA} of ≈ 0.9 W/cm^2) targets. Under these conditions, Pt-specific power densities of ≈ 0.5 $\text{g}_{\text{Pt}}/\text{kW}$ can be obtained with optimized MEAs (first row in Table I),¹⁹ corresponding to catalyst costs of $\approx \$18/\text{kW}$ (assuming $\approx \$35/\text{g}_{\text{Pt}}$ for a Pt/C catalyst). This does not meet the stringent automotive cost requirements, with catalyst cost targets of $\ll \$10/\text{kW}$, equivalent to < 0.2 $\text{g}_{\text{Pt}}/\text{kW}$.

While clearly the Pt cathode loading must be reduced to the 0.1 $\text{mg}_{\text{Pt}}/\text{cm}^2$ level to meet the < 0.2 $\text{g}_{\text{Pt}}/\text{kW}$ target, it would lead to a 40 mV loss in cell voltage,^{2,19} which for efficiency reasons is not acceptable, thereby requiring improved cathode catalysts. Platinum-cobalt alloys (PtCo/C) and other Pt alloys were demonstrated to yield an activity improvement by a factor of 2 compared to Pt/C,¹⁹ and implementation of these catalysts enables a lowering of the cathode Pt-loading to 0.1 $\text{mg}_{\text{Pt}}/\text{cm}^2$ at an overall performance loss of 20 mV. In this case (second row of Table I), the Pt-specific power density reduces to 0.19 $\text{g}_{\text{Pt}}/\text{kW}$, yielding a catalyst cost of $\approx \$7/\text{kW}$. While this is acceptable

(continued on next page)

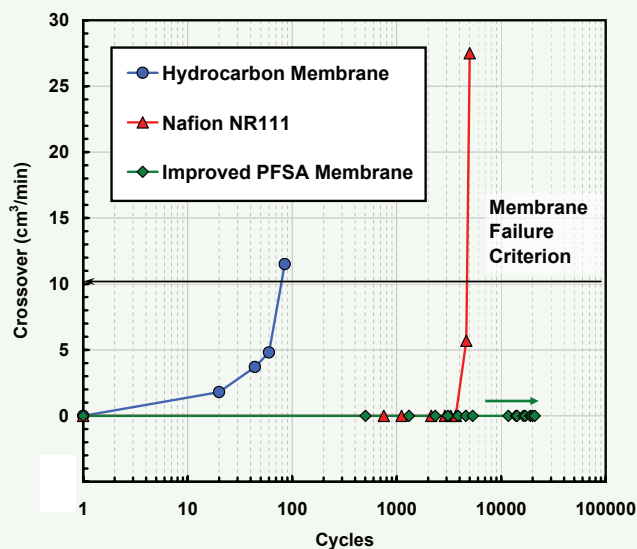


FIG. 4. MEA crossover leak vs. number of RH cycles for catalyst coated membranes based on different 25 μm thick membranes: two PFSA membranes and one hydrocarbon membrane. RH cycle conditions: 150% RH, 2 min \leftrightarrow 0% RH, 2 min cycles (air/air) at 80°C using 50 cm^2 catalyst coated membranes and carbon paper diffusion media. Membrane gas crossover leak rates (in sccm) were determined with air at a pressure differential of 20 kPa across the membrane.

TABLE I. MEA power densities, P_{MEA} , and Pt-specific power densities, P_{Pt} , in state-of-the-art MEAs (anode: 0.05 $\text{mg}_{\text{Pt}}/\text{cm}^2$). H_2/air operation at nominal conditions of 80°C and 150 kPa_{abs}.¹⁹

Catalyst activity	Cathode loading ($\text{mg}_{\text{Pt}}/\text{cm}^2$)	P_{MEA} at 0.65 V (W/cm^2)	P_{Pt} at 0.65 V ($\text{g}_{\text{Pt}}/\text{kW}$)
Pt/C	0.4	0.91	0.48
2x Pt/C	0.1	0.78	0.19
4x Pt/C	0.1	0.91	0.17

from a catalyst cost viewpoint, Pt-alloy catalysts with a fourfold activity enhancement are desirable to improve the overall MEA power density to $\approx 0.9 \text{ W/cm}^2$ (third row of Table I), to minimize the cost pressure on the other stack components. Even though the above arguments (for more details see Ref. 19) support a clear technology pathway to meet automotive PEFC catalyst cost requirements, the durability of these catalysts under automotive usage profiles must still be demonstrated.

Electrocatalyst Durability

Similar to membranes, catalysts must also survive harsh transient (load-cycling) operation of a vehicle. While Pt catalysts are stable at the low electrode potentials occurring at the anode electrode [0 to 0.05 V vs. the reversible hydrogen electrode potential (RHE)], Pt dissolution poses significant concerns at the high electrode potentials occurring in the cathode electrode ($\approx 0.7\text{--}0.95 \text{ V}$ vs. RHE). Recent focus on catalyst durability has helped advance the understanding of the detailed mechanism of Pt surface area loss in PEFCs. Similar to the work done in PAFC development,^{20,21} Ferreira *et al.*²² used transmission electron microscopy (TEM) analyses of significantly degraded MEA cross sections to understand Pt surface area loss mechanism and concluded that coarsening of Pt particles occurred via two different processes: (1) a *nanometer-scale* Ostwald-ripening process where smaller Pt particles dissolve in the ionomer phase and redeposit on larger Pt particles that are separated by a few nanometers for a well-dispersed catalyst; and (2) a *micrometer-scale* diffusion process, where dissolved Pt species diffuse in the ionomer phase and subsequently precipitate in the ionomer phase of the electrode or the membrane (close to the cathode/membrane interface) via reduction of Pt ions with cross-over hydrogen from the anode.

In this section, we discuss the impact of steady state and voltage-cyclic operation on Pt and Pt-alloy stability. We also extend the discussion to evaluate if Pt dissolution will limit high temperature (120°C), low RH (25%) operation if and when a suitable membrane becomes available.

Pt dissolution at steady-state potential. – Bindra *et al.*²³ reported substantial Pt solubility (using Pt foil)

in hot concentrated phosphoric acid ($176\text{--}196^\circ\text{C}$) in the potential range between 0.8 and 0.95 V (vs. RHE), consistent with Pt being oxidized to soluble Pt^{2+} ions, with the solubility increasing by a decade for increase in voltage by $2.303RT/2F$, where R is the universal gas constant, T is temperature, and F is the Faraday constant. Increasing Pt dissolution with potential is also reported for highly dispersed Pt on carbon-support (Pt/C) at temperatures relevant to PEFCs (80°C) in 0.5 M sulfuric acid in the potential range between 0.9 and 1.1 V (vs. RHE),²² even though the potential-dependence was not consistent with Nernstian behavior.

Two 15-cell short stacks (800 cm^2 active area) were operated for 2,000 h at steady state with H_2 -air (constant reactant flows corresponding to a stoichiometry of $s=2/2$ at 0.2 A/cm^2 at 80°C (fully humidified) and 150 kPa_{abs} to examine the effect of potential on Pt dissolution in an operating fuel cell. Gore Series-5510[®] catalyst-coated membranes (CCM) with 0.4 $\text{mg}_{\text{Pt}}/\text{cm}^2$ Pt/C loadings were sandwiched between carbon-fiber-paper-based diffusion media (Toray Inc., Japan) with proprietary hydrophobic treatments and microporous layers. Figure 5a shows the voltages of two different short stacks operated at open-circuit voltage (OCV) (square symbols, $\sim 0.97 \rightarrow \sim 0.93 \text{ V}$ vs. RHE) and at a constant current of 0.2 A/cm^2 (triangle symbols, at $\sim 0.78 \rightarrow \sim 0.73 \text{ V}$ vs. RHE). A linear approximation of the voltage decay rates for those two stacks yields 20 and 25 $\mu\text{V/h}$ for stack operation at OCV and 0.2 A/cm^2 , respectively. These rather similar voltage decay rates are surprising as the potential dependence of Pt solubility would suggest lower decay rates for lower cathode potentials as observed for PAFC stacks.^{20,21}

In situ cyclic voltammetry measurements at 25°C (using fully humidified H_2/N_2 and 20 mV/s) were carried out intermittently through the life of the stacks to determine the electrochemical Pt surface area in the cathode (evaluated in terms of $\text{m}^2/\text{g}_{\text{Pt}}$),¹⁹ and data are shown in Fig. 5b. These data resolve the apparent inconsistency and demonstrate that the Pt area loss of the stack operated at OCV is much more pronounced vs. the Pt area loss for operation at 0.2 A/cm^2 . This result is in qualitative agreement with Pt

dissolution potential-dependence found in PAFC stacks,^{20,21} sulfuric acid,²² and phosphoric acid.²³ The voltage degradation rate of 20 $\mu\text{V/h}$ at OCV is consistent with the 22 $\mu\text{V/h}$ which one would calculate from the Pt surface area loss, S_{Pt} , over 2,000 h (Fig. 5b)

$$\left. \frac{\partial E_{\text{cell}}}{\partial t} \right|_{i, i_0, T, P_i} \approx \left. \frac{\partial E_{\text{cathode}}}{\partial t} \right|_{i, i_0, T, P_i} = \frac{-b \log \left(\frac{S_{\text{Pt}}(t)}{S_{\text{Pt}}(t=0)} \right)}{\Delta t} \quad \text{Eq. [1]}$$

where Δt is the duration of the experiment and b is the Tafel slope of the oxygen reduction reaction with a value of 0.070 V at 80°C (*i.e.*, a value of $2.303RT/F$).¹⁹ The derivation of Eq. 1 (from Eq. 8 in Ref. 3) is based on the assumption that the Pt-area normalized specific activity (*i.e.*, i_s in units of $[\text{A}/\text{cm}^2_{\text{Pt}}]$) of the cathode catalyst is independent of the platinum area decay over time (in other words, the exchange current density, i_0 , changes insignificantly). The latter was confirmed in a recent study by Yu *et al.*,²⁴ in which less than 25% variation of i_s was found for largely varying S_{Pt} -values produced by Pt-dissolution/sintering of both Pt/C and PtCo/C catalysts (due to voltage-cycling). The voltage degradation rate of 25 $\mu\text{V/h}$ observed for the stack operated at 0.2 A/cm^2 is significantly larger than the 10 $\mu\text{V/h}$ estimated using Fig. 1 and data in Fig. 5b. The difference is attributable to mass transport losses.

Pt and Pt-alloy dissolution and mass activity loss at steady state potential. – As described earlier, catalysts with enhanced mass activity are required to meet long term catalyst cost requirements. One major challenge in the implementation of Pt-transition metal alloy catalyst, such as PtCo/C, is the need to maintain their high mass activity advantage vs. Pt/C for 5,500 h in a vehicle. A large active-area short stack consisting of MEAs made with Pt/C and PtCo/C cathodes was operated for 1,000 h to test long term Pt-alloy stability under steady state conditions with H_2 -air (stoichiometric reactant flows of $s = 2/2$) at 80°C (fully humidified) and 150 kPa_{abs} . The anodes for all MEAs (Pt and PtCo cathodes) were made from $\approx 50 \text{ wt } \%$ Pt/C. Half the MEAs of the stack were made of $\approx 50 \text{ wt } \%$ Pt/C cathodes and the other half were made of $\approx 50 \text{ wt } \%$ PtCo/C cathodes (note that PtCo/C is used to refer to a carbon-supported platinum-cobalt alloy and is not meant to indicate any specific composition). All the catalysts for the stack were supplied

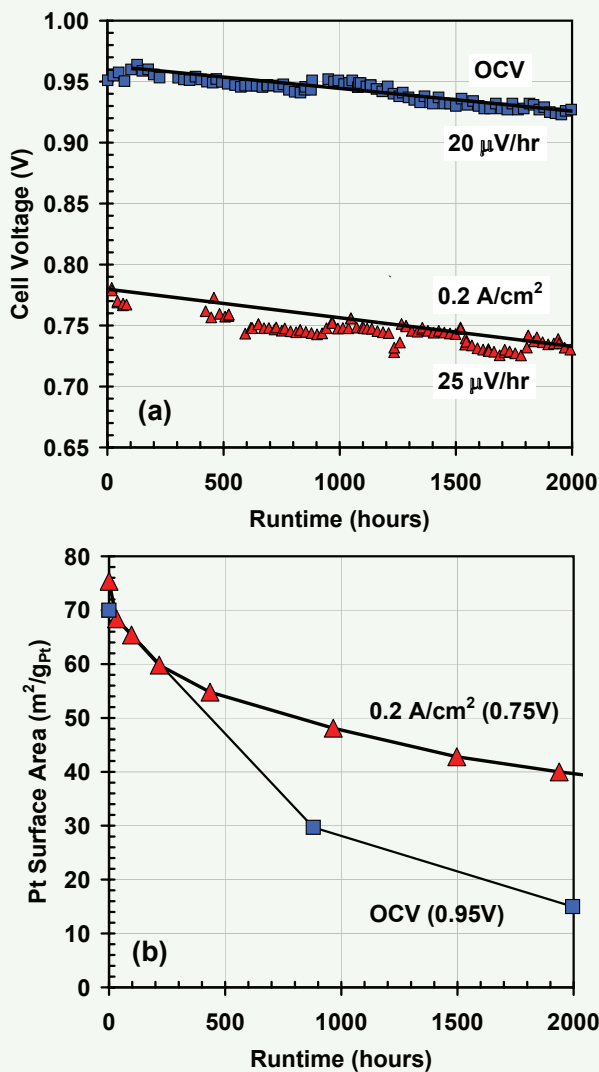


Fig. 5. (a) Cell voltage and (b) Pt surface area as a function of stack runtime. Stacks were operated with H_2/air ($s = 2/2$) at 80°C , $150 \text{ kPa}_{\text{abs}}$, and 100% RH. Surface areas were determined by cyclic voltammetry using H_2/N_2 at 25°C and 20 mV/s .

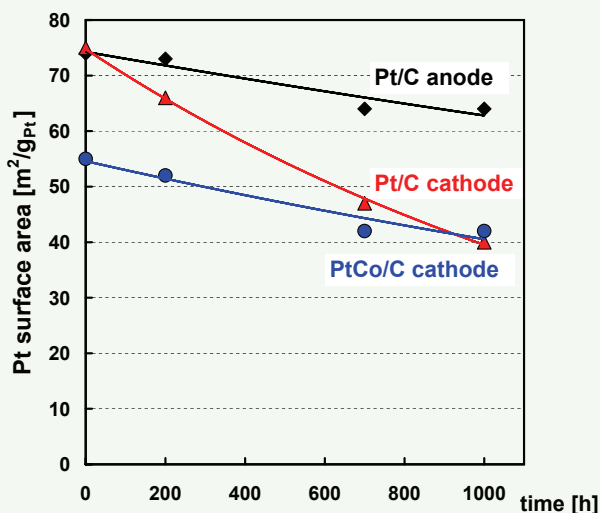


Fig. 6. Pt surface area loss of (♦) $\approx 50 \text{ wt } \%$ Pt/C anode, (▲) $\approx 50 \text{ wt } \%$ Pt/C cathode, and (●) $\approx 50 \text{ wt } \%$ PtCo/C cathode. Stacks were operated with H_2/air ($s = 2/2$) at 80°C , $150 \text{ kPa}_{\text{abs}}$, and 100% RH. Surface areas were determined by cyclic voltammetry using H_2/N_2 at 25°C and 20 mV/s .

by Tanaka Kikinzoku Kogyo (TKK). The PtCo/C catalyst used in the test was preleached by the supplier using a proprietary procedure (durability benefits of using preleached Pt-alloy catalysts are described in detail elsewhere¹⁹).

Cyclic voltammetry at room temperature was used to monitor the change in Pt surface area over the life of the stack (see Fig. 6). Higher Pt surface area of Pt/C electrodes at the beginning-of-life can be attributed to its smaller particle size (2-3 nm) as compared to PtCo/C catalysts (4-6 nm). As expected, due to the potential dependence of Pt dissolution, Pt surface area loss on the anode (diamond symbols, Pt/C) is significantly lower than that on the cathode (triangle symbols, Pt/C), an observation which was noted in several previous studies.^{25,26} Although Pt/C initially has higher Pt surface area, both Pt/C and PtCo/C achieve similar Pt surface area at the end-of-testing (1,000 h). Whether the slower decay of Pt electrochemical surface area observed for the PtCo/C alloy is due to its larger particle size (*i.e.*, low surface energy) and/or its intrinsically superior stability over Pt/C is still unclear.

To assess activity changes over time, catalyst specific activity, i_s [$\mu\text{A}/\text{cm}^2_{\text{Pt}}$], and mass activity, i_m [$\text{A}/\text{mg}_{\text{Pt}}$], measurements¹⁹ were made at 0.9 V over the life of the stack in pure hydrogen and oxygen with reactant flow set at stoichiometry of 2 and 9, respectively. The operating conditions for the catalyst activity measurement were identical to the stack durability conditions (80°C , $150 \text{ kPa}_{\text{abs}}$, 100% RH). It can be seen in Fig. 7a that the specific activity of Pt/C stays constant over life, whereas that of PtCo/C decreases by a factor 1.8 in 1,000 h. In absence of clear fundamental understanding of the mechanism, specific activity degradation of PtCo/C catalyst is generally speculated to be due to slow loss of the transition metal (Co in this case) over a long period of time. Co was found in the membrane at end-of-test using electron probe microanalysis (EPMA). Figure 7b shows that the mass activity of the two catalysts decreased at a similar rate. Since the specific activity of Pt/C remains constant over time, the decrease in mass activity is due purely to loss in Pt surface area attributable to dissolution. The advantage of lower Pt surface area loss for PtCo/C is partially counteracted by a decrease in specific activity, giving the net

(continued on next page)

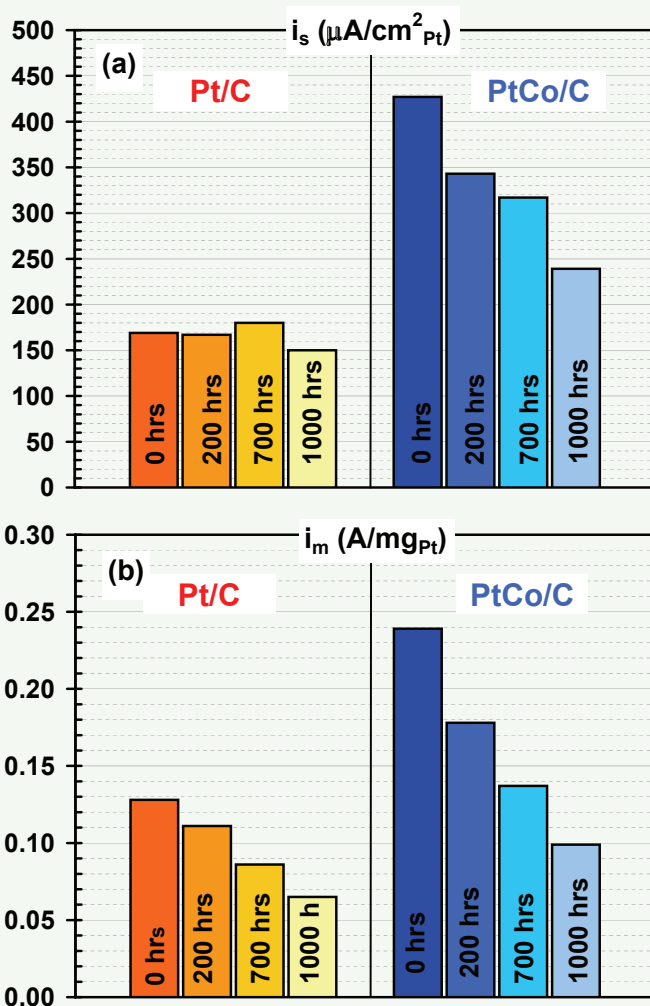


Fig. 7. Changes in (a) specific activity and (b) mass activity of ≈ 50 wt % Pt/C and ≈ 50 wt % PtCo/C catalysts (defined at 0.9 V, 80°C, and 100 kPa_{abs} H₂ and O₂) in short stacks operated under 80°C, 150 kPa_{abs}, and 100% RH.

result of similar mass activity loss as Pt/C. Due to the combined effect of Pt surface area and specific activity changes over time for both catalysts, the benefit in mass activity of PtCo/C vs. Pt/C reduces from a factor of 1.9 at the beginning-of-life to 1.6 at end-of-test. Such intrinsic degradation of Pt-alloy catalyst may result in unacceptable performance loss during the life of a vehicle. The need for long term stability of Pt-alloy warrants increased effort toward fundamental understanding of specific activity loss in Pt-alloy catalysts leading to development of stable catalysts via modifications in materials and synthesis processes.

Pt dissolution under potential cycling. – It is known that voltage cycling of polycrystalline and carbon-supported Pt in aqueous acids at room temperature leads

to accelerated Pt dissolution rates compared to extended holds at constant potentials.^{27,28} Although the exact nature of this phenomenon is unknown, it is hypothesized that the interruption/reduction of relatively corrosion resistant, steady state oxide/hydroxide coverage of Pt during voltage transients to low potentials leads to accelerated Pt dissolution in subsequent voltage cycling to high potentials. The analogous phenomenon has been observed in PEFCs and was reported for the first time in the public literature by Patterson,²⁹ showing accelerated Pt area loss of a H₂/air PEFC cathode electrode subjected to square-wave voltage cycles between 0.87 and 1.20 V (65°C and 60 s/cycle). Darling and Meyers³⁰ have recently developed and reported an initial numerical model describing the voltage cycling induced Pt area loss by assuming a

potential dependent dissolution of metallic Pt ($\text{Pt} \leftrightarrow \text{Pt}^{2+} + 2\text{e}^-$, *i.e.*, a $2.303RT/2F$ potential dependence), chemical dissolution of Pt oxide ($\text{PtO} + 2\text{H}^+ \leftrightarrow \text{Pt}^{2+} + \text{H}_2\text{O}$), and surface tension driven growth of Pt nanoparticles. This model based on an Ostwald ripening mechanism has been subsequently refined,³¹ yielding a reasonable prediction of Patterson's voltage cycling data.²⁹

Analysis of various standardized US vehicle drive cycles such as Federal Urban Drive Cycle (FUDS), US06, and others reveals that a vehicle experiences roughly 300,000 load (voltage) cycles between peak power (0.7 iR-free V) and idle (0.9 iR-free V) through its life of 5,500 h. A simple test was developed to measure the impact of peak power to idle load cycling on Pt surface area loss and to provide a benchmark for catalyst voltage-cycling durability which would be projected to satisfy automotive requirements. The test consists of cycling a 50 cm² MEA under H₂/air (constant flow of stoichiometry 2/2 at 2 A/cm²) at desired temperature and RH between 0.7 and 0.9 iR-free voltage (30 s hold at each potential) combined with occasional evaluation of the remaining Pt surface area, S_{Pt} , using cyclic voltammetry. The long term vehicle performance degradation target of ≤ 3 $\mu\text{V}/\text{h}$ over 5,500 h requires an absolute voltage loss of ≤ 17 mV over the projected 300,000 large voltage cycles (0.7 \leftrightarrow 0.9 iR-free voltage); using Eq. 1 and assuming only minor changes in specific activity caused by Pt dissolution/sintering (see discussion above), this translates to a requirement of less than 40% loss in Pt surface area in 300,000 voltage cycles.

Pt vs. Pt-alloy dissolution under potential cycling. – Yu *et al.*²⁴ recently reported enhanced stability of PtCo between 0.87 and 1.2 V voltage cycling. We have also evaluated the stability of PtCo catalyst under our proposed benchmark voltage cycling conditions (0.7 \leftrightarrow 0.9 iR-free voltage). Figure 8 shows normalized Pt surface area of ≈ 50 wt % Pt/C and ≈ 30 wt % PtCo/C over 30,000 voltage cycles at 80°C, 100% RH, a 500 h test. To gauge the feasibility of the catalyst to meet the vehicle life requirement of 300,000 cycles, we can extrapolate the Pt surface area by one order of magnitude in cycle number. The acceleration of Pt dissolution under voltage cycling may be observed by comparing voltage cycling Pt surface area loss of Pt/C to that under steady state OCV. At steady state (Fig. 5b,

OCV data), a 10% Pt surface area loss is observed over 250 h as compared to 70% area loss in V-cycling test (Fig. 8, Pt/C data) in 30,000 cycles, also amounting to 250 h at 0.9 V. Under fully humidified conditions, Pt loses most of its surface area after 300,000 voltage cycles and leads to high and unacceptable performance degradation. In contrast, loss of surface area of PtCo is low and extrapolation to 300,000 cycles suggests that the catalyst will meet vehicle end-of-life performance targets, as long as there is no significant loss in specific activity over 5,500 h of transient operation. Because the proposed voltage cycling test does not take into account the effect of long term operation on catalyst specific activity, it is also important to evaluate the impact of cycling on catalyst activity.

Impact of RH and temperature on Pt dissolution under Pt cycling. – It is widely reported that Pt is found in the membrane after long term operation^{20,21,32} and voltage cycling of the cathode.^{22,24,29} TEM analyses of degraded MEA cross sections²² unambiguously confirm that Pt diffuses in the ionomer phase of the electrode toward the membrane and is reduced by H₂ permeating through the membrane at or close to the cathode/membrane interface. Based on this model, the diffusion coefficient of Pt ions in the ionomer phase is expected to strongly impact the rate of Pt area loss. While no Pt diffusion coefficient data in PFSA are available in the literature, one might expect a behavior analogous to the proton diffusion coefficient in PFSA, which is reduced by an order of magnitude as the RH is reduced from 100 to 25%.³³ While this may seem to be a far-fetched assumption, the following data illustrate the suggested impact of RH on the rate of Pt area loss.

The RH dependence of Pt surface area loss was evaluated for a \approx 50 wt % Pt/C catalyst under the voltage cycling protocol at 80°C as described in the previous section. As seen in Fig. 9, Pt surface area loss is largely mitigated by operating the cell at 25% RH (diamond symbols) as compared to 100% RH (circular symbols). This finding is consistent with the hypothesis that, besides the kinetics of Pt dissolution itself, Pt cation diffusion in the ionomer phase plays a major role in determining the overall rate of the Pt surface area loss process.

In a previous article,⁵ we discussed the advantages reflected

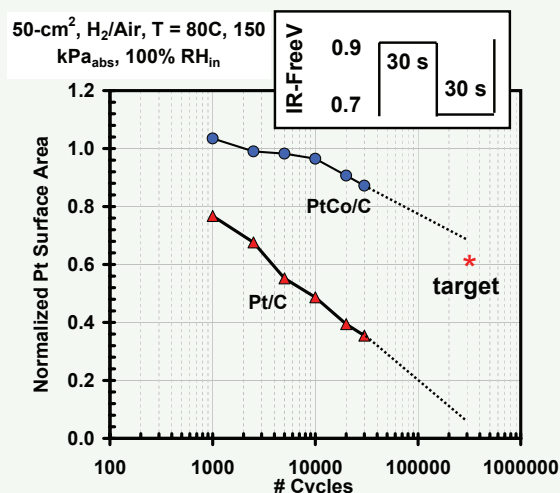


Fig. 8. Pt surface area loss of (\blacktriangle) \approx 50 wt % Pt/C, and (\bullet) \approx 30 wt % PtCo/C as a function of the number of potential cycles between 0.7 and 0.9 V (iR-free potentials) in H₂/air at 80°C and 100% RH.

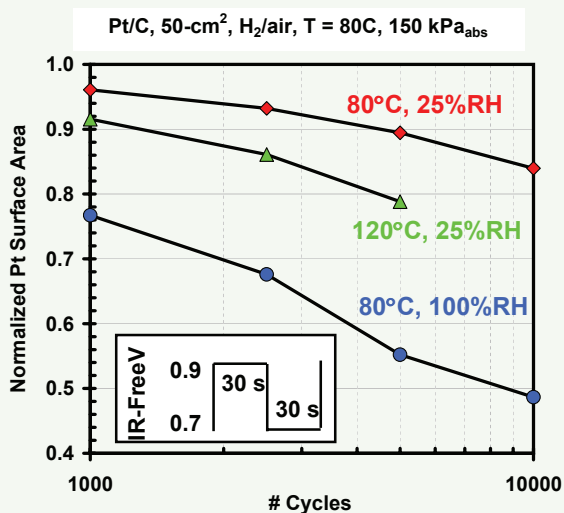


Fig. 9. Impact of RH and high temperature operation on Pt surface area loss of Pt/C as a function of potential cycles (same as Fig. 8). (\bullet) 80°C, 100% RH, (\blacklozenge) 80°C, 25% RH, (\blacktriangle) 120°C, 25% RH.

in reduction of system complexity by implementing a high temperature (120°C), low RH (25% RH) membrane. However, based on Pt solubility data at 25 and 196°C and subsequent interpolation, the same authors cautioned that high temperature operation could cause half the Pt to dissolve in a little over 100 h of operation.⁶ A voltage cycling experiment was performed to test catalyst stability at desired high temperature, low RH operation (120°C, 25% RH) using PFSA ionomer in the membrane and the electrode. Figure 9 shows Pt surface area loss data for Pt/C at 120°C, 25% RH (triangle symbols). At 25% RH, although Pt surface area loss at 120°C is slightly higher than that at 80°C, the losses are much lower as compared to those at 80°C 100%

RH. Pt surface area loss at high temperature and low RH is expected to be still lower for Pt-alloy catalysts. Our available data under automotive relevant transient conditions thus suggest that Pt dissolution should not be a hindrance to implementation of high temperature (120°C) membranes if they can operate at low RH (also required to achieve required system simplicity). Catalyst support durability (next section) under high temperature, low RH conditions must still be evaluated.

In summary, losses due to Pt dissolution can be mitigated by implementing Pt-transition metal alloys and low-RH systems. Both requirements are directionally correct in that Pt alloys are required

(continued on next page)

to increase mass activity and low-RH systems offer reduced system complexity and increased flexibility in system design and operation. Both aspects of this future direction also help bring down stack/system costs significantly. Therefore, to address catalyst durability requirements, increased research effort should be directed toward increasing Pt alloy long term stability and improving their mass activity gain over Pt/C catalysts. In addition, catalyst durability would also be improved via the development of low-RH membranes (low or high temperature, 80-120°C) since low RH operation reduces the rate of Pt area loss.

Catalyst-Support Durability

Besides the dissolution/sintering of the active metal discussed above, the corrosion of the catalyst supports may be a critical issue in PEFCs under certain operating conditions. In phosphoric acid fuel cells (PAFCs) which operate at $\approx 200^\circ\text{C}$, corrosion rates of the commonly used high surface area carbon supports (*e.g.*, Vulcan-XC72 and Ketjen black) were unacceptably high, necessitating the implementation of more corrosion-resistant graphitized carbon supports.^{34,35} Due to the significantly lower operating temperature of PEFCs ($\approx 80^\circ\text{C}$), it has largely been assumed that carbon-support corrosion would be negligible and, consequently, current MEAs are based on Vulcan-XC72 and Ketjen black carbon supports. This assumption is correct for cathode potentials in the normal PEFC operating range (iR-corrected cathode potentials between 0.85 and 0.6 V), but the following analysis demonstrates that automotive applications involve cathode potential ranges which far exceed the stability region of these standard carbon supports even at 80°C .

PEFCs in automotive applications undergo an estimated 30,000 startup/shutdown cycles over the life of a vehicle, which can lead to short term potential excursions of the cathode electrode to 1.2-1.5 V due to H_2 /air fronts in the anode compartment.³⁶ At these high potentials, corrosion rates of standard carbon supports are high, leading to large voltage degradation rates. While operating and controls strategies were shown to effectively mitigate voltage excursion beyond 1.2 V,³⁶ passive shutdown of a PEFC stack (*i.e.*, removal of H_2 upon shutdown, leading to air in both the

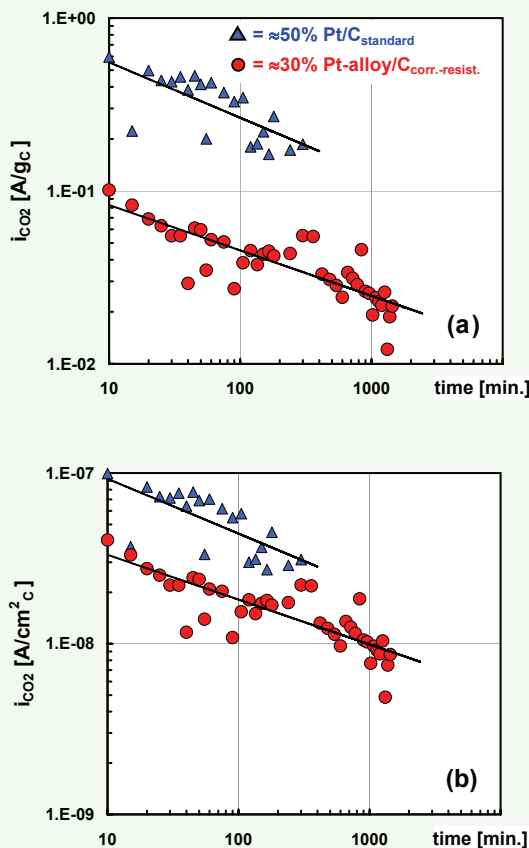


Fig. 10. CO_2 corrosion currents vs. time of cathode electrodes (50 cm^2 MEAs) potentiostated in N_2 to 1.2 V (vs. a 100% H_2 anode) at 95°C (100% RH, $120\text{ kPa}_{\text{abs}}$) determined by CO_2 on-line analysis. CO_2 currents are normalized to either (a) carbon mass, or (b) carbon BET surface area ($\approx 600\text{ m}^2/\text{g}_\text{C}$ for the Pt catalyst and $\approx 250\text{ m}^2/\text{g}_\text{C}$ for the Pt-alloy catalyst).

anode and the cathode) establishes anode and cathode potentials of up to $\approx 1.2\text{ V}$ (*i.e.*, the thermodynamic air potential). Assuming that the stack remains at this condition at 80°C for approximately 10 s per shutdown (time required to significantly cool the stack), catalyst-support stability at 1.2 V is required for an accumulated time of $\approx 100\text{ h}$ over the life of the vehicle, with a maximum allowable performance loss of $<30\text{ mV}$ at $1.5\text{ A}/\text{cm}^2$ ($<1\text{ }\mu\text{V}/\text{cycle}$ target). A similarly critical operating condition is the long idle time of automotive stacks, *i.e.*, the time when only idle auxiliary load power is drawn from the stack, resulting in cathode potentials of $\approx 0.9\text{ V}$ and above (depending on the particular usage profile, this may amount to several thousand hours over vehicle life).

The following experimental data and analysis serves to assess the stability of different carbon supports, at either $\approx 100\text{ h}$ at 1.2 V or thousands of hours at 0.9 V, with the goal of determining whether improved catalyst supports are required for automotive applications.

The carbon corrosion rates of two different catalysts, a Pt catalyst on a standard high surface area carbon support and a Pt alloy (TKK, 3 wt % PtCo) on a corrosion resistant carbon support, are shown in Fig. 10a under an accelerated testing condition of 95°C . Mass normalized CO_2 currents were obtained (assuming $4e^-$ reaction) by on-line gas analysis of the N_2 effluent from cathode electrodes potentiostated at 1.2 V in a 50 cm^2 MEA operated with fully humidified H_2/N_2 (anode/cathode). As previously observed for uncatalyzed carbon blacks,³⁷ the logarithm of the CO_2 current decays linearly with the logarithm of time (the physical origin of this behavior is still unknown). Clearly, the mass normalized CO_2 current of the catalyst with corrosion resistant carbon is almost one order of magnitude lower than that of a standard carbon support, related in part to its lower Brunauer-Emmett-Teller (BET) surface area ($\approx 250\text{ m}^2/\text{g}_\text{C}$ vs. $\approx 600\text{ m}^2/\text{g}_\text{C}$) as well as to its lower intrinsic corrosion rate (*i.e.*, its lower BET surface area normalized current, see Fig. 10b). The latter phenomenon is consistent with former comparisons

between graphitized and non-graphitized carbons in both alkaline³⁸ and phosphoric acid³⁴ electrolytes, which indicated two to four times lower intrinsic corrosion rates for graphitized carbons.

Detailed studies of the temperature, potential, and time-dependence of the CO₂ corrosion current of the ≈50 wt % Pt/C_{standard} catalyst (data not shown) revealed that the corrosion kinetics follow

$$i_{CO_2} \propto 10^{E/TS} e^{-E_a/(RT)} t^{-m} \quad [2]$$

with a Tafel slope of 150 mV/decade, an activation energy (E_a) of 67 kJ/mol, and a time-decay exponent (m) of 0.30 (independent of temperature and potential). Using these kinetics, we estimated the carbon weight loss at the above outlined conditions of 0.9 V/80°C (vehicle idle conditions) and 1.2 V/80°C (startup/shutdown condition) vs. time. As is shown in Fig. 11, the ≈50 wt % Pt/C_{standard} catalyst is projected to lose ≈15% of its weight in only 20 h at 1.2 V and will not survive the required 100 h at 1.2 V; similarly, at the idle condition of ≈0.9 V, it will experience ≈5% weight loss over several thousand hours. While these values represent rough estimates, it is likely that this catalyst will not satisfy automotive carbon support durability requirements (see below). A similar projection was made for the ≈30 wt % Pt alloy/C_{corr.-resist.} catalyst, assuming the above values for Tafel slope and activation energy, and is shown as the red curve in Fig. 11. While its advantage over the ≈50 wt % Pt/C_{standard} catalyst is obvious, whether the projected carbon weight loss under the given conditions is small enough to not induce mass transport related voltage degradation is still to be determined.

To resolve the latter question, experiments were conducted where cathode catalysts were subjected to potential hold experiments at 1.2 V and 80°C (100% RH) for different time periods, with subsequent evaluation of their H₂/air performance under fuel cell relevant conditions (outlined in Fig. 12). After 20 h at 1.2 V, the H₂/air performance of the ≈50 wt % Pt/C_{standard} cathode decreases 30 mV at 1.5 A/cm², and the increasing voltage loss with increasing current density clearly indicates the onset of mass-transport losses induced by carbon corrosion. At 30 h exposure to 1.2 V, mass-transport

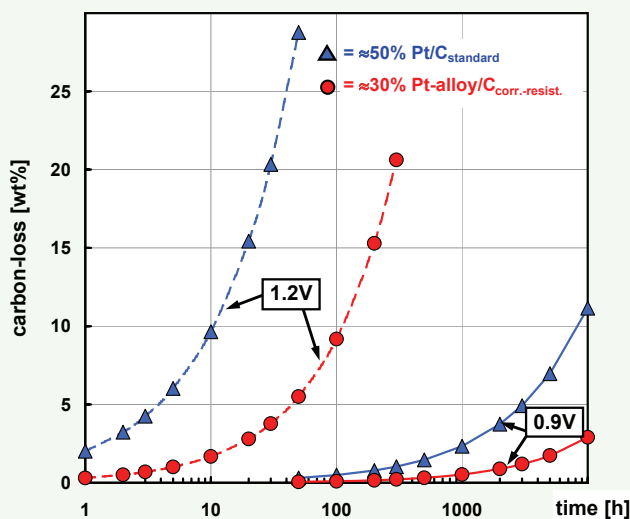


Fig. 11. Carbon weight loss vs. time for two different catalysts at both 0.9 V (idle condition) and 1.2 V (approximate air/air potential) and 80°C (100% RH, 120 kPa_{abs}). Predictions are based on the data in Fig. 10, assuming a Tafel slope of 150 mV/decade, an activation energy of 67 kJ/mol, and the same i_{CO_2} vs. time dependence as shown in Fig. 10 for each catalyst.

losses are unacceptably high, clearly indicating that a standard carbon support will not meet automotive requirements. On the contrary, the ≈30 wt % Pt alloy/C_{corr.-resist.} cathode shows no decrease in performance even after 100 h exposure to 1.2 V; unfortunately, its beginning-of-life performance is much lower than what one would expect based on its mass activity measured in H₂/O₂, related to the fact that optimization of electrodes with corrosion-resistant support is still in its infancy. It should be noted that the observed losses for the ≈50 wt % Pt/C_{standard} cathode are even larger at more humidified conditions, but since diffusion-medium corrosion is difficult to decouple from electrode corrosion at higher humidity levels, our proposed materials screening test is conducted at the lower

humidity condition. Based on our present observations, carbon weight losses between 5 and 10% lead to unacceptably large performance degradation under most operating conditions, thereby implying that standard carbon supports (Vulcan-XC72 and Ketjen black) do not satisfy automotive requirements (see Fig. 12) with respect to either startup/shutdown cycles or prolonged idle conditions.

In summary, development and implementation of highly dispersed Pt-alloy catalysts on corrosion-resistant supports (e.g., graphitized carbon blacks) are required to meet automotive durability requirements. This not only necessitates significant R&D efforts by catalyst developers, but also requires focused efforts by

(continued on next page)

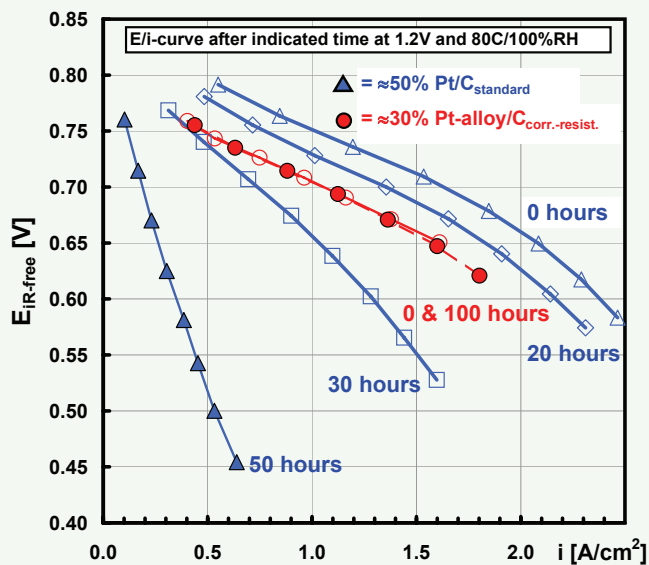


FIG. 12. Impact of accelerated carbon support corrosion on the E/i performance curves of 50 cm² MEAs with both a ≈50% Pt/C_{standard} and a ≈30 wt % Pt alloy/C_{corr.-resist.} cathode catalyst. MEA cathodes were subjected to accelerated carbon support corrosion at 1.2 V and 80°C for the indicated times, using fully humidified H₂/N₂ gas streams (anode/cathode). H₂/air (stoichiometric flows of s = 3/3) performance curves were recorded at 80°C, 50% RH, and 150 kPa_{abs} (MEAs with ≈25 μm membranes, catalyst loadings of 0.2-0.4 mg_{Pt}/cm², and SGL-25BC diffusion media).

MEA suppliers to integrate these new materials into high performing H₂/air MEAs. Our currently suggested benchmark for determining whether catalyst support materials meet automotive requirements is a potential hold at 1.2 V followed by evaluation of H₂/air performance. At the same time, however, we are investigating whether 1.2 V is an appropriate estimate for the air/air potential or whether the actual air/air potential is lower than the 1.2 V thermodynamic limit (viz., a lower mixed potential produced by simultaneous carbon support corrosion and oxygen reduction). It may be the case that voltage cycling has a similar effect on carbon support corrosion as it has on Pt dissolution, *i.e.*, cycling may accelerate carbon corrosion. In the former case, our present requirements for catalyst support stability are too high, while in the latter case they may not be stringent enough. These are open questions which we hope to have resolved in the near future.

Summary

The currently known material set for PEFCs, *i.e.*, PFSA membranes and Pt-based catalysts, are in principle

able to meet the cost requirements for high volume automotive applications. To enable automotive fuel cell commercialization, further materials optimization and improved understanding of the currently observed degradation mechanisms are needed. Specifically, future R&D efforts directed at membrane and catalyst materials development should focus on

- Development of low-RH (0.1 S/cm at 25-50% RH) membranes with a main operating temperature of 60-80°C and short time temperature excursions up to *ca.* 100°C. Development of high temperature (120°C) membranes that offer 0.1 S/cm at 25% RH or less is a longer term goal. Membranes should not swell by over a factor of 2 vs. dry volume when placed in boiling water. This must be achieved without compromising chemical degradation stability and RH-cycling stability.
- Development of Pt-alloy cathode catalysts with improved activity compared to Pt/C and the current generation of PtCo/C, with a long term goal of fourfold mass activity over Pt/C. Simultaneously, these new catalysts must maintain both their mass activity for extended

voltage cycling and their specific activity over long term operation.

- Development of more stable catalyst supports that have improved corrosion resistance at high potentials (*i.e.*, under start-stop and idle conditions). Reasonably high BET surface area (on the order of >100 m²/g) is desired to enable good dispersion of the active phase (*e.g.*, Pt surface areas of >50 m²/g_{Pt}).

In addition, work focused in the following areas is needed to provide theoretical support to the materials development efforts:

- Understanding of the physical limits of materials based on the sulfonic acid conduction mechanism to enable the development of low-RH membranes operating at 60-120°C.
- Fundamental understanding of the morphology of membranes and its impact on their mechanical properties, particularly in terms of fatigue, long term creep, and structural changes under cyclic conditions (*i.e.*, cyclic variations of temperature and RH).
- Understanding of the fundamental chemical degradation mechanisms of ionomers used both in the electrode and in the membrane, including the dependence on electrode materials and design.
- The likelihood of developing cathode catalysts with improved mass activity and durability (both Pt-based and non-Pt catalysts), would be largely increased if accompanied by strong fundamental molecular modeling approaches. These models must incorporate aspects of both activity enhancement and dissolution stability and should be complemented by fundamental electrocatalysis work on model surfaces.
- The implementation of new catalysts in high performance H₂/air MEAs is still largely based on trial-and-error and more an art than a science. Therefore, fundamental research on electrode characterization (*e.g.*, ionomer distribution, correlation between support structure and electrode performance, etc.) and modeling of mass transport phenomena in electrodes is desired to enable timely implementation of new catalyst/catalyst-support materials.

Finally, we suggest the use of the material characterization tests described here as screening tools

for automotive fuel cell materials development: (i) membrane conductivity vs. RH and water uptake, (ii) membrane RH-cycling test, (iii) catalyst voltage cycling test, and, (iv) support corrosion test at 1.2 V. While these test procedures may not be perfect and may change

somewhat over time, we feel that they provide a reasonable evaluation and benchmarking for new materials.

Acknowledgments

We thank Mike Scozzafava, John Doyle, and Alain Bergeron for

preparing MEA samples and Mary Ann Sweikart and Jason Willey for experimental data. We also acknowledge many fruitful discussions with Fredrick W. Wagner. ■

References

1. K. Strasser, in *Handbook of Fuel Cells – Fundamentals, Technology, and Applications*, W. Vielstich, A. Lamm, H. A. Gasteiger, Editors, Vol. 4, p. 1201, John Wiley & Sons, Chichester, U.K. (2003).
2. H. A. Gasteiger, J. E. Panels, and S. G. Yan, *J. Power Sources*, **127**, 162 (2004).
3. H. A. Gasteiger, W. Gu, R. Makharia, M. F. Mathias, and B. Sompalli, in *Handbook of Fuel Cells*, Vol. 3, p. 593.
4. S. Cleghorn, J. Kolde, and W. Liu, in *Handbook of Fuel Cells*, Vol. 3, p. 566.
5. M. F. Mathias and H. A. Gasteiger, in *Proton Conducting Membrane Fuel Cells III*, M. Murthy, T. F. Fuller, J. W. Van Zee, and S. Gottesfeld, Editors, PV 2002-31, p. 1, The Electrochemical Society Proceedings Series, Pennington, NJ (2005).
6. M. Mathias, H. Gasteiger, R. Makharia, S. Kocha, T. Fuller, T. Xie, and J. Pisco, *Prepr. Pap.-Am. Chem. Soc., Div. Fuel Chem.*, **49**(2), 471 (2004).
7. M. Doyle and G. Rajendran, in *Handbook of Fuel Cells*, Vol. 3, p. 351.
8. DuPont Nafion® Fuel Cell Division, Fayetteville, NC.
9. G. Alberti, M. Casciola, L. Massinelli, and B. Bauer, *J. Membrane Sci.*, **185**, 73 (2001).
10. Z. Bai, L. D. Williams, M. F. Durstock, and T. D. Dang, *Polym. Prepr.*, **45**(1), 60 (2004).
11. D. Masten and A. D. Bosco, in *Handbook of Fuel Cells*, Vol. 4, p. 714.
12. J. S. Wainright, M. H. Litt, and R. F. Savinell, in *Handbook of Fuel Cells*, Vol. 3, p. 436.
13. L. Rubatat, A. L. Rollet, G. Gebel, and O. Diat, *Macromolecules*, **35**, 4050 (2002).
14. A. B. LaConti, M. Hamdan, and R. C. McDonald, in *Handbook of Fuel Cells*, Vol. 3, p. 647.
15. C. Paik, T. Skiba, V. Mittal, S. Motupally, and T. Jarvi, Abstract 771, V. Mittal, C. Paik, and S. Motupally, Abstract 772, C. Urgeghe, A. Battisti, Y. Garsany, J. Ziegelbauer, S. Mukerjee, A. Gulla, and R. Allen, Abstract 790, S. Hommura, K. Kawahara, and T. Shimohira, Abstract 803, M. Inaba, H. Yamada, J. Tokunaga, and A. Tasaka, Abstract 1506, T. Takeshita, F. Miura, and Y. Morimoto, Abstract 1511, The Electrochemical Society Meeting Abstracts, Vol. 2005-1, Quebec City, Canada, May 15-20, 2005.
16. E. Endoh, S. Terazano, H. Widjaja, and Y. Takimoto, *Electrochem. Solid-State Lett.*, **7**, A209 (2004).
17. D. E. Curtin, R. D. Lousenberg, T. J. Henry, P. C. Tangeman, and M. E. Tisack, *J. Power Sources*, **131**, 41 (2004).
18. Y. H. Lai, C. Mittelsteadt, C. Gittleman, D. Dillard, in *Proceedings of FUELCELL2005, Third International ASME Conference on Fuel Cell Science, Engineering, and Technology*, Ypsilanti, MI (2005).
19. H. A. Gasteiger, S. S. Kocha, B. Sompalli, and F. T. Wagner, *Appl. Catal. B: Env.*, **56**, 9 (2005).
20. J. Aragane, T. Murahashi, and T. Odaka, *J. Electrochem. Soc.*, **135**, 844 (1988).
21. J. Aragane, H. Urushibata, and T. Murahashi, *J. Appl. Electrochem.*, **26**, 147 (1996).
22. P. J. Ferreira, G. J. la O', Y. Shao-Horn, R. Makharia, and H. A. Gasteiger, *J. Electrochem. Soc.*, Submitted.
23. P. Bindra, S. J. Clouser, and E. Yeager, *J. Electrochem. Soc.*, **126**, 1631 (1979).
24. P. Yu, M. Pemberton, and P. Plasse, *J. Power Sources*, **144**, 11 (2005).
25. T. Tada, in *Handbook of Fuel Cells*, Vol. 3, p. 481.
26. M. S. Wilson, F. H. Garzon, K. E. Sickafus, and S. Gottesfeld, *J. Electrochem. Soc.*, **140**, 2872 (1993).
27. R. Woods, in *Electroanalytical Chemistry*, A. J. Bard, Editor, Vol. 9, Marcel Dekker, New York (1976).
28. K. Kinoshita, J. T. Lundquist, and P. Stonehart, *J. Electroanal. Chem. Interfacial Electrochem.*, **48**, 157 (1973).
29. T. Patterson, in *Fuel Cell Technology Topical Conference Proceedings*, AIChE, p. 313 (2002).
30. R. M. Darling and J. P. Meyers, *J. Electrochem. Soc.*, **150**, A1523 (2003).
31. R. M. Darling and J. P. Meyers, *J. Electrochem. Soc.*, **152**, A242 (2005).
32. J. Xie, D. L. Wood, D. M. Wayne, T. A. Zawodzinski, P. Atanassov, and R. L. Borup, *J. Electrochem. Soc.*, **152**, A104 (2005).
33. S. Gottesfeld and T. Zawodzinski, in *Advances in Electrochemical Science and Engineering*, R. C. Alkire, H. Gerischer, D. M. Kolb, and C. W. Tobias, Editors, Vol. 5, p. 195, John Wiley & Sons-VCH, Weinheim, Germany (1997).
34. K. Kinoshita, *Carbon: Electrochemical and Physicochemical Properties*, John Wiley & Sons, New York (1988).
35. D. A. Landsman and F. J. Luczak, in *Handbook of Fuel Cells*, Vol. 4, p. 811.
36. C. A. Reiser, L. Bregoli, T. W. Patterson, J. S. Yi, J. D. Yang, M. L. Perry, and T. D. Jarvi, *Electrochem. Solid-State Lett.*, **8**, A272 (2005).
37. K. Kinoshita and J. Bett, *Carbon*, **11**, 238 (1973).
38. P. N. Ross and M. Sattler, *J. Electrochem. Soc.*, **135**, 1464 (1988).

About the Authors

MARK F. MATHIAS is a Technical Fellow in General Motor's Fuel Cell Activities Division. He oversees research in the areas of alternative membrane, diffusion media, and plate materials. He can be reached at mark.mathias@gm.com.

ROHIT MAKHARIA is a Project Engineer in GM's Fuel Cell Activities Division. He leads efforts to understand and mitigate electrode degradation. He can be reached at rohit.makharia@gm.com.

HUBERT A. GASTEIGER is a Technical Fellow in GM's Fuel Cell Activities Division. He oversees research in the areas of catalyst development and durability. He can be reached at hubert.gasteiger@gm.com.

JASON J. CONLEY (jason.conley@gm.com), **TIM FULLER** (timothy.fuller@gm.com), **CRAIG GITTLEMAN** (craig.gittleman@gm.com), **SHYAM S. KOCHA** (shyam.kocha@gm.com), **DANIEL MILLER** (daniel.

miller@gm.com), **TAO XIE** (tao.xie@gm.com), **SUSAN G. YAN** (susan.yan@gm.com), and **PAUL T. YU** (taichiang.yu@gm.com) are members of the GM Fuel Cell Activities Research Staff. **CORTNEY K. MITTELSTEADT** (cmittelsteadt@ginerinc.com) is Associate Director of Energy Conversion at Giner Electrochemical Systems in Newton, MA.